Solid-state NMR and thermodynamic investigations on LiBH4-LiNH2 system

Solid-state NMR and thermodynamic investigations on $LiBH_4$-$LiNH_2$ system

A.Wolczyk, E.Pinatel, M.Chierotti, C.Nervi, R.Gobetto, M.Baricco*

Department of Chemistry and NIS, University of Turin, Via P. Giuria 9, I-10125 Turin (Italy)

Abstract

In this paper, $Li_2(BH_4)(NH_2)$ and $Li_4(BH_4)(NH_2)_3$ compounds were prepared through different synthesis approaches (ball milling, annealing treatment and liquid quenching) and characterized by X-ray diffraction and solid-state NMR. The thermal analysis of samples with various $(LiBH_4)_{1-x}(LiNH_2)_x$ compositions ($0 \leq x \leq 1$) have been performed by High Pressure DSC. Lattice constants, chemical shifts and relative phase stability obtained by DFT turned out in good agreement with experimental data. On the basis of a combination of ab-initio calculations and experimental data, a thermodynamic assessment of the $LiBH_4$-$LiNH_2$ system has been obtained using the Calphad method. $Li_2(BH_4)(NH_2)$ has been identified as a metastable phase and a peritectic melting of $Li_4(BH_4)(NH_2)_3$ compound has been established.

Keywords: complex hydrides, High Pressure DSC, solid-state NMR, ab-initio, Calphad

*corresponding author:

Prof. Marcello BARICCO
Department of Chemistry and NIS
University of Turin
Via P.Giuria, 9
I-10125 TORINO (Italy)
Tel. + 39 011 670 7569
Mob. +39 366 7877947
Fax. + 39 011 670 7855
e-mail: marcello.baricco@unito.it

Introduction

Hydrogen storage materials based on complex hydrides have been investigated in recent years with the goal to improve hydrogen gravimetric density and to match thermodynamic requirements necessary for dehydrogenation reactions with equilibrium close to ambient conditions [1]. In fact, complex hydrides show a much higher gravimetric hydrogen density with respect to transition metal hydrides [2]. $LiBH_4$-$LiNH_2$ system, because of the high gravimetric hydrogen densities of both complex hydrides, has been widely investigated for solid state hydrogen storage [3].

Complex hydrides are of special interest also for electrochemical energy storage as novel solid state ion conductors and anode conversion materials [4]. $LiBH_4$ exhibits lithium superionic conduction (>10^{-3} S/cm at 126 °C) due to a structural transition from the orthorhombic low-temperature (LT) to the hexagonal high-temperature (HT) phase at about 110 °C, which allows Li^+ ions migration along specific crystallographic directions. So, it has been suggested as solid-state electrolyte for Li-ion batteries [5]. Lithium ionic conduction in $LiNH_2$ displays extremely low values at room temperature (<10^{-8} S/cm), slightly increasing upon heating (about 5×10^{-6} S/cm at 127 °C) [6], suggesting a limited ionic mobility in the structure [7]. Orimo *et al.* [8,9] have reported a lithium fast-ion conductions in $Li_2(BH_4)(NH_2)$ and $Li_4(BH_4)(NH_2)_3$ compounds, constituted by Li^+ cation and BH_4^- and NH_2^- anions [10]. $Li_2(BH_4)(NH_2)$ and $Li_4(BH_4)(NH_2)_3$ melt at temperatures around 86 °C and 186 °C, respectively, indicating the possible enhancement of total ion conductivity in low temperature ranges [11]. Indeed, $Li_2(BH_4)(NH_2)$ exhibits a fast lithium ion conductivity (2×10^{-4} S/cm) even at room temperature (RT), which is 4 orders of magnitude higher than that of $LiBH_4$. Upon heating, the Li^+ ion conductivity reaches a value up to 6×10^{-2} S/cm at 104 °C. $Li_4(BH_4)(NH_2)_3$ is also characterized by a high Li^+ ion conductivity at RT (around 2×10^{-4} S/cm), which increases up to 1×10^{-3} S/cm at about 96 °C [8].

Several studies investigated the thermal decomposition on Li-B-N-H compounds and different pseudo-binary phase diagrams have been suggested for the $LiBH_4$-$LiNH_2$ system [12,13,14,2]. Meisner *et al*. [12], together with the presence of $Li_2(BH_4)(NH_2)$ and $Li_4(BH_4)(NH_2)_3$ compounds,

reported the synthesis of a new quaternary hydride in the Li-B-N-H quaternary phase diagram with the approximate composition $LiB_{0.33}N_{0.67}H_{2.67}$, having a theoretical hydrogen content of 11.9 wt %. They suggested a metastable phase diagram, showing an eutectic point at about 80 °C for $(LiBH_4)_{0.8}(LiNH_2)_{0.20}$ composition. Singer *et al.* [13] performed in-situ X-ray Diffraction experiments and proposed a pseudo-binary phase diagram for the $(LiBH_4)_{1-x}(LiNH_2)_x$ system in the $0.5 \leq x \leq 0.75$ composition range for temperatures up to 250 °C, showing an eutectic point. Although authors points out that both composition and temperature of the eutectic were not yet determined, they are expected to fall within the displayed ranges (x = 0.556÷0.6 and 50÷80 °C, respectively). In addition, an off-stoichiometry composition range has been established for the $Li_4(BH_4)(NH_2)_3$ compound. Combining in-situ diffraction experiments with a DSC study and physical observations on various compositions, Anderson *et al.* [10] established that the $(LiBH_4)_{1-x}(LiNH_2)_x$ system shows an eutectic point close to the x = 0.33 composition. They suggested that $Li_2(BH_4)(NH_2)$ is a thermodynamically metastable compound and it decomposes into $Li_4(BH_4)(NH_2)_3$ and $LiBH_4$ upon heating. Later, Borgschulte *et al.* [2] adapted the pseudo-binary phase diagram of $LiBH_4$-$LiNH_2$ system from ref. [14].

In this work, various samples in $LiBH_4$-$LiNH_2$system were prepared by different synthesis routes (i.e. ball milling, annealing treatment and liquid quenching) and a detailed examination of the phase stability was performed through a combination of X-ray diffraction (XRD), solid-state nuclear magnetic resonance (solid-state NMR) and High Pressure Differential Scanning Calorimetry (HP_DSC) experimental techniques. Ab-initio calculations allowed the relative stability of crystal phases, together with lattice constants and solid-state NMR ^{1}H, ^{7}Li, ^{11}B and ^{15}N chemical shifts to be estimated. All these parameters showed a good agreement with experimental findings. Coupling ab-initio calculations with a Calphad assessment, an equilibrium pseudo-binary $LiBH_4$-$LiNH_2$ phase diagram has been obtained, showing $Li_2(BH_4)(NH_2)$ compound as a metastable phase and a peritectic melting for $Li_4(BH_4)(NH_2)_3$ compound.

Experimental and Computational Methods

Mixtures of $LiBH_4$ and $LiNH_2$ from commercially available powders ($LiNH_2$: Aldrich, 95% purity; and $LiBH_4$: Rockwood, 97% purity) were handled in an inert atmosphere (N_2) glovebox to avoid oxidation and reaction with ambient water.

Mixtures of $(LiBH_4)_{1-x}(LiNH_2)_x$ were synthesized for compositions x = 0.50 and 0.75, to form $Li_2(BH_4)(NH_2)$ and $Li_4(BH_4)(NH_2)_3$ compounds. For ball milled (BM) samples, a hardened steel ball to powder ratio 10:1 was used inside O-ring sealed jars. Samples were milled with a SPEX 8000 Mixer/Mill for 300 min. Other samples have been firstly grounded manually in agate mortar for 5 minutes and then annealed (AT) from room temperature to T = 120 °C (for 1:1 mixture) and to T = 250 °C (for 1:3 mixture) in HP_DSC, at 10°C/min under 10 bars of H_2. Cooling process down to RT was performed under the same conditions. $Li_2(BH_4)(NH_2)$ and $Li_4(BH_4)(NH_2)_3$ compounds were also prepared by liquid quenching (QU). A proper amount of $LiBH_4$ and $LiNH_2$ were heated in a glass tube under Ar pressure of 2 bar. After heating up to 190°C for 1:1 mixture and up to 110 °C for 1:3 mixture, the samples were annealed for 3 hours and then quenched (QU) through immersing the reaction tube in iced water and finally re-grounded under argon to reduce powder size.

Samples were characterized at room temperature by using X-ray diffraction (XRD) using a Panalytical X-pert (Cu Kα) in trasmission geometry using 0.8 mm glass capillary. A Rietveld refinement of diffraction patterns has been perfomed using MAUD (Materials Analysis Using Diffraction) program [15].

HP_DSC measurements were performed using a DSC 204 by Netzsch running inside a glove box. For each measurement, about 10 mg of sample weresealed in an aluminum crucible under inert atmosphere. 1:1 and 1:3 mixtures of $LiBH_4$:$LiNH_2$ were heated twice up to 120 °C and 250 °C, respectively, in order to follow the formation of the compounds. In addition, both pure starting complex hydrides and six different values of their combination A (x = 0.15), B (x = 0.33), C (x = 0.50), D (x = 0.65), E (x = 0.75) and F (x = 0.85), where x is a composition of the form $(LiBH_4)_{1-x}(LiNH_2)_x$, have been examinated. All samples were heated at 10 °C/min from room temperature up

to 250 °C (except $LiNH_2$, which was heated up to 380 °C because of its higher temperature of melting), kept at the maximum temperature for 30 min, and thereafter cooled to RT, continiously under 10 bar of H_2 pressure.

Solid-state NMR measurements were run on a Bruker Advance II 400 instrument operating at 400.23, 155.54, 128.41 and 40.56 MHz for ^{1}H, ^{7}Li, ^{11}B and ^{15}N, respectively. ^{1}H magic-angle spinning (MAS) spectra were acquired in a 2.5 mm probe with a spinning speed of 32 kHz using the DEPTH sequence for suppressing the probe background signal [90° pulse = 1.8 μs; recycle delays = 0.5-3 s; 16 transients]. ^{7}Li, ^{11}B and ^{15}N spectra were recorded at room temperature at the spinning speed of 12 kHz with cylindrical 4 mm o.d. zirconia rotors with sample volume of 80 μL. For ^{7}Li and ^{11}B MAS spectra, single-pulse excitation (SPE) or DEPTH (for suppressing the probe background signal) sequences were used [90° pulse = 3.75 (^{11}B) and 2.35 μs (^{7}Li); recycle delays = 0.4 (^{11}B) or 50–140 s (^{7}Li); 16 transients]. ^{15}N CPMAS spectra were acquired with a ramp cross-polarization pulse sequence (contact time = 4 ms; a ^{1}H 90° pulse = 3.05 s, recycle delays = 0.5-3 s, 16000–20000 transients) with two-pulse phase modulation (TPPM) decoupling scheme (rf field = 75 kHz). The ^{1}H, ^{7}Li, ^{11}B and ^{15}N chemical shift scales were calibrated using adamantane (^{1}H signal at 1.87 ppm), 1 M aqueous LiCl (^{7}Li signal at 0.0 ppm), $NaBH_4$ (^{11}B signal at −42.0 ppm with respect to $BF_3{\cdot}Et_2O$) and $(NH_4)_2SO_4$ (^{15}N signal at μ = 355.8 ppm with respect to CH_3NO_2) as external standards, respectively.

Periodic lattice calculations based on density-functional theory (DFT) were performed by means of Quantum Espresso version 5.1.2. [16]. The Generalized Gradient Approximation (GGA) functional PW86PBE, [17] with the inclusion of the exchange-hole dipole moment (XDM) [18] dispersion correction method for accurate model of the weak interactions was used in all calculations. XDM dispersion energies were calculated adopting the damping parameters optimized for the inorganic systems under study (a1 = 1.2153 and a2 = 2.3704). Experimental data for $LiBH_4$ [19], $LiNH_2$ [20], $Li_2(BH_4)(NH_2)$ [21] and $Li_4(BH_4)(NH_2)_3$ [21] were used as starting structures for molecular

geometry and cell optimizations. Calculations were performed adopting the Kresse-Joubert Projected Augmented Wave pseudopotentials [22]. A cut-off of 60 Ry was used for structural optimizations. The Brillouin zones were automatically sampled with the Monkhorst–Pack scheme [23], in a similar approach as previously described [24]. Geometry optimization and NMR chemical shift calculations were performed for $LiBH_4$, $LiNH_2$, $Li_2(BH_4)(NH_2)$ and $Li_4(BH_4)(NH_2)_3$, with a grid mesh of 2×3×2, 6×6×3, 2×2×5 and 2×2×2, respectively. The NMR chemical shifts were calculated using a 120 Ry energy cut-off by the GIPAW method [25]. The theoretical absolute magnetic shielding (σ) values were converted into ^{1}H chemical shifts (δ) relative to the absolute magnetic shielding of the reference substance $LiBH_4$ (σ = 31.19), computed at the same level as a weighted mean of three set of magnetically non equivalent ^{1}H resonances (σ = 31.13, 31.60, 31.02, with relative intensities of 1:1:2). For practical purposes, the ^{1}H chemical shifts were reported against TMS (the experimental value of δ ^{1}H for $LiBH_4$ vs. TMS is –0.2 ppm), in a similar way as previously described [26]. $LiBH_4$ data have been used also for referencing ^{11}B (σ = 139.60, δ = –41.8 ppm) and ^{7}Li (σ = 90.17, δ = –0.91 ppm, against LiCl 1M), whereas ^{15}N has been referenced to $LiNH_2$ (σ = 224.14, δ = –18.6 ppm).

Thermodynamic modelling has been carried out according to the Calphad approach [27]. This method is based on a parametric analytical description of the Gibbs Free Energy (GFE) for each phase as a function of temperature (*T*), pressure (*p*) and composition (*x*). The parameters are obtained by a least square procedure, starting from experimental data and theoretical ab-initio calculations for thermochemical properties available for the investigated system. The obtained database can then be used to evaluate the stable phases for a given set of conditions (*T*, *p* and *x*) by minimizing the GFE. In order to have a consistent database to be compared and integrated with those available in the literature, as customary, pure elements in their stable phases at 25 °C and 1 atm were used as reference state (SER, Standard Element Reference). Since pressure dependence is negligible for condensed phases, its contribution to the GFE was considered only for the gas phase, assuming an ideal behaviour.

Results and Discussion

The XRD patterns of $(LiBH_4)_{1-x}(LiNH_2)_x$ samples prepared from different routes forcompositions x = 0.50 and x = 0.75 are shown in *Figure 1*. For x = 0.50 composition (*Figure 1a*), a phase fraction of 70 wt % and 14 wt % of 1:1 compound have been obtained from BM and AT synthesis, respectively. For BM sample, lattice constants for the rhomboherdal compound turnedout equal to *a* = 14.456 Å and *c* = 9.206 Å, whereas they are *a* = 14.449 Å and *c* = 9.218 Å for AT sample. Remaining phases are emerging $Li_4(BH_4)(NH_2)_3$ compound (29 wt % in case of BM, and 63 wt % for AT), as well as unreacted $LiBH_4$ (23 wt% in case of AT) or traces of unreacted $LiNH_2$ (in case of BM). From these results, it appears clear that ball milling and annealing treatment are inadequate methods for preparing a pure $Li_2(BH_4)(NH_2)$ phase. Following the quenching route, an almost pure $Li_2(BH_4)(NH_2)$phase (95 wt %, rest 5 wt% of unreacted $LiBH_4$), with lattice constants *a* = 14.457 Å and *c* = 9.226 Å, has been obtained, as shown in *Figure 1a* for QU sample.

For all samples, the values of lattice constants are in good agreement with those reported in the literature [21,3,10], as shown in *Table 1*. For x = 0.75 composition (*Figure 1b*), following different synthesis routes, a high content of $Li_4(BH_4)(NH_2)_3$ compound has been obtained, corresponding toabout 78 wt % in case of BM (rest 22 wt % of unreacted $LiNH_2$), 80 wt % in case of AT (rest 6 wt % and 14 wt % for unreacted $LiBH_4$ and $LiNH_2$, respectively) and 90 wt % in case of QU (rest 10 wt % of unreacted $LiNH_2$). It is worth noting that, according to ref. [28], after heating a $LiBH_4$:$LiNH_2$ mixture in a 1:3 molar ratio at around 100 °C (i.e. near the orthorombic-hexagonal structural transition temperature of $LiBH_4$), a repeated grinding and annealing at 180 °C was necessary to obtain a single phase. In the present work, similar results were obtained after quenching from 190 °C (data not shown) and from 110 °C (*Figure 1b*), confirming an off-stoichiometry composition range for the $Li_4(BH_4)(NH_2)_3$ compound [13]. The lattice constant obtained for the cubic phase after Rietveld refinement was equalto *a* = 10.666 Å for the BM, *a* = 10.657 Å for AT and *a* = 10.656 Å for QU sample, in good agreement with values reported in the

literature [21,10,29,30], as shown in *Table 1*. In all samples, the presence of unreacted $LiNH_2$ has been observed, because of the off-stoichiometry of the $Li_4(BH_4)(NH_2)_3$ compound. In conclusion, results of XRD analysis shows an easier synthesis for the $Li_4(BH_4)(NH_2)_3$ compounds with respect to $Li_2(BH_4)(NH_2)$, which can be obtained only following the QU route, suggesting a metastability for this phase [21]. So, in order to clarify this point, thermal analysis measurements have been performed.

The formation of $Li_2(BH_4)(NH_2)$ and $Li_4(BH_4)(NH_2)_3$ compounds has been followed by HP_DSC and the results are shown in *Figure 2*. For each measurement, two heating-cooling cycles have been performed. For the 1:1 mixture, a maximum temperature of 125 °C has been selected, as shown in *Figure 2a*. In both heating curves, an endothermic peak can be observed at around 90÷110 °C, being as a broad bamp for the first rampand a sharp peak for the secondone. This peak can be associated to the melting of the $Li_2(BH_4)(NH_2)$ phase, which was already formed during heating in the first run, appearing more clearly in the second cycle. In both cycles, this peak is followed by a small endothermic signal at around 110 °C, associated to the LT-to-HT phase transformation of unreacted $LiBH_4$. On cooling ramps, in both cycles a small exothermic signal (at about 105 °C) is accountable for the reversible phase transformation of unreacted $LiBH_4$. It is followed at about 80 °C by a sharp exothermic peak, which can be ascribed to the solidification of the $Li_2(BH_4)(NH_2)$ phase or, more likely, to an eutectic transition. For the 1:3 mixture, a maximum temperature of 250 °C has been reached, as shown in *Figure 2b*. In the first heating curve, an endothermic peak at about 90÷110 °C is followed by an exothermic one. This sequence can be associated to the melting of $Li_2(BH_4)(NH_2)$ phase formed at low temperature, followed by the formation of $Li_4(BH_4)(NH_2)_3$ compound, due to the reacion of the liquid with unreacted $LiNH_2$ still present in the mixture. A broad endothermic peak is following, starting at about 200 °C and ending with a sharper signal at about 225 °C, which can be associated to the progressive melting of the $Li_4(BH_4)(NH_2)_3$ compound. On cooling, an exothermic peak at about 200 °C can be observed, due to the solidification of the $Li_4(BH_4)(NH_2)_3$ compound, followed by a smaller peak at about 85 °C, possibily due to a residual

eutectic solidification. The HP_DSC signals in the second cycle are rather similar to those of the first one, but only a single endothermic peak is observed at about 90 °C on heating, because the crossing of the eutectic line. Interestingly, a strong undercooling of the liquid can be observed, as evidenced by the exothermic peak at about 180 °C in the cooling trace.

HP_DSC measurements werealso carried out on mixtures with various compositions in the $(LiBH_4)_{1-x}(LiNH_2)_x$ ($0 \leq x \leq 1$) system and results are shown in *Figure 3*. The bottom thermogram in *Figure 3* is showing the phase transformation of $LiBH_4$, from LT to HT phase, at around 110°C [31]. A second sharp endothermic peak, at around 275°C, is responsible forthe melting of the compound. The top HP_DSC trace up to 380 °C in *Figure 3* is related to pure $LiNH_2$, where only the peak due tomelting is visible, starting at about 355 °C. A corresponding enthalpy of melting (ΔH_m) of 14.3 kJ/mol has been obtained, in good agreement with the value already reported in the literature, ΔH_m = 13.3 ± 0.2 kJ/mol at 366 °C [32]. The addition of $LiNH_2$ (sample A, x = 0.15) does not change the temperature for LT-to-HT phase transformation of $LiBH_4$, as shown in the HP_DSC trace in *Figure 3*, suggesting that no solubility of NH_2^- anion occurs in $LiBH_4$. Melting takes place in a wide temperature range on heating, as suggested by the barely visible endothermic HP_DSC peak. For further addition of $LiNH_2$ to $LiBH_4$ (sample B, x = 0.33), the eutectic composition suggested in ref. [14] is considered. A rather broad endothermic peak is observed in temperature range 80÷110 °C (marked with *x* in the figure), related to a continuous melting of phase mixtures formed during heating at lower temperatures, followed by a tiny endothermic peak, likely due to the LT-to-HT phase transformation of a small amount of unreacted $LiBH_4$ still present in the mixture. No more peaks can be observed in the DSC trace, suggesting that a full liquid phase was present at higher temperatures. For thecomposition corresponding to $Li_2(BH_4)(NH_2)$ compound (sample C, x = 0.50), a liquid phase is formed on heating (peak *x* in the figure) due to the melting of the compound formed at lower temperatures, as already shown in *Figure 2a*. At higher temperatures, it can react with remaining $LiNH_2$ to form $Li_4(BH_4)(NH_2)_3$ compound. As a consequence, a second broad endothermic peak is observed in the HP_DSC trace, due to its progressive melting. As already

observed in *Figure 2a*, a tiny signal due to the LT-to-HT phase transformation of unreacted $LiBH_4$ is still observable. For compositions in between $Li_2(BH_4)(NH_2)$ and $Li_4(BH_4)(NH_2)_3$ compounds (sample D, x = 0.65), no peaks have been observed up to the LT-to-HT phase transformation of $LiBH_4$. Immediately after this event, a clear exothermic peak suggests the formation of $Li_4(BH_4)(NH_2)_3$ phase. A complicated endothermic signal due to melting is then observed in the 200÷220 °C temperature range, without further signal up to 300 °C. For the mixture corresponding to $Li_4(BH_4)(NH_2)_3$ phase (sample E, x = 0.75), the compound is slightly formed on heating in the HP_DSC, as shown by a small exothermic signal at about 100 °C (marked as *y* in the figure). Up to 300 °C, only a sharp endothermic signal is observed at about 220 °C, due to the melting of the compound. Finally, a further addition of $LiNH_2$ phase (sample F, x = 0.85) gives rather similar results. Even in this case, a broad exothermic peak (marked as *y* in the figure) is observed around 100 °C, due to the formation of the $Li_4(BH_4)(NH_2)_3$ compound, followed by its melting at about 220 °C. Characteristic temperatures of phase trasnformations for various compositions have been identified in HP_DSC traces, as evidenced in *Figure 3*, to be used for the assesment of the phase diagram.

A further characterization of the samples obtained from quenching (QU) synthesis route has been performed by ^{1}H, ^{7}Li and ^{11}B MAS and ^{15}N CPMAS solid-state NMR. As already shown in *Figure 1*, 1:1 and 1:3 mixtures are basically composed by $Li_2(BH_4)(NH_2)$ and $Li_4(BH_4)(NH_2)_3$ compounds. Spectra for pure parent complex hydrides ($LiBH_4$ and $LiNH_2$) have been also collected for comparison. The corresponding results are shown in *Figure 4* and *Figure 5* and corresponding chemical shifts are listed in *Table 2*.

^{1}H MAS spectra (*Figure 4*, top) give information on the purity of the samples. They are both characterized by two overlapped resonances. The x = 0.50 sample shows one sharper resonance around -0.2 ppm (FWHM δ591 Hz) and one broader peak centred at -0.3 ppm (FWHM ~1937 Hz) attributed to BH_4^- and NH_2^- anions, respectively [33]. Data have been obtained from a peakanalysis, as shown in *Figure 4*. An integral signals ratio of 2:1 agrees well with the stoichiometry of the

$Li_2(BH_4)(NH_2)$ compound. Similary, the x = 0.75 sample displays a signal around -0.2 ppm (FWHM ~550 Hz) and another at -0.9 ppm (FWHM ~1937 Hz) in ratio 2:3 for BH_4^- and NH_2^- anions, as expected for the $Li_4(BH_4)(NH_2)_3$ compound. The ^{15}N CPMAS spectra (*Figure 4*, down) are characterized by a single NH_2^- resonance around -19.0 ppm. The shift of the ^{15}N signals in 1:1 and 1:3 mixtures compared to pure $LiNH_2$ is due to the different environment of the NH_2^- anion. As expected, its environment is much different in the case of 1:1 mixture, where the relative amount of NH_2^- anion is smaller with respect to 1:3 mixture, which results in being more similar to pure $LiNH_2$. Small shifts are observed in the ^{11}B and ^{7}Li MAS spectra for samples obtained from 1:1 and 1:3 mixtures with respect to those of the pure reagents, as shown in *Figure 5* top and bottom, respectively. The width of the spinning sidebands (ssb) pattern in the ^{7}Li and ^{11}B spectra is related to the symmetry of the environment around the Li^+ and BH_4^- ions, respectively. Concerning the ^{7}Li MAS spectra, the environment around the Li^+ cation is similar for 1:1 and 1:3 mixtures. It is characterized by a low symmetry and resembles that observed in pure $LiNH_2$ rather than that obtained for pure $LiBH_4$, which is highly symmetric. Concerning the ^{11}B MAS spectra, in the case of 1:1 mixture, the Li^+ cation distribution around the BH_4^- units is slightly asymmetric, resembling that of pure $LiBH_4$. In fact, if the BH_4^- anion is assumed to have a perfect tetrahedral structure, the asymmetry derives only from the Li^+ distribution around it. On the other hand, in the case of 1:3 mixture, the Li^+ distribution seems to be much more symmetric, as evidenced by the smaller pattern of ssb.

Results of periodic plane wave calculations on $LiBH_4$, $LiNH_2$, $Li_2(BH_4)(NH_2)$ and $Li_4(BH_4)(NH_2)_3$ gave excellent agreement between the experimental and the optimized structures, with small deviations of lattice parameters and cell volumes, as shown in *Table 1*. Calculations performed at 0 K for mixed compounds agree nicely with experimental results reported in ref. [21], whereas more recent reports [3,10] provided a slightly higher value for the *c* parameter of the unary cell of $Li_4(BH_4)(NH_2)_3$. The optimized geometries of $Li_2(BH_4)(NH_2)$ and $Li_4(BH_4)(NH_2)_3$ compounds were

found to have lower energy than the mixture $LiBH_4$ + $LiNH_2$ and $LiBH_4$ + 3 $LiNH_2$ by 6.6 and 13.9 kJ/mol, respectively. For $Li_4(BH_4)(NH_2)_3$ compound, our theoretical prediction for the energy of reaction between pure complex hydrides is higher than that previously reported [34] (6 kJ/mol) and fits reasonably with the value obtained by Siegel *et al.* [35] at 0 K (11.3 kJ/mol). To our knowledge, calculations of $Li_2(BH_4)(NH_2)$ geometries have not been reported in the literature; as already observed [21], there are large voids present in the $Li_2(BH_4)(NH_2)$ structure, and likely the much dense structure of $Li_4(BH_4)(NH_2)_3$ makes this phase slightly more stable. From the obtained thermodynamic parameters, it turns out that the formation reaction of $Li_2(BH_4)(NH_2)$ from $LiBH_4$ and $Li_4(BH_4)(NH_2)_3$ has a slightly positive energy value, suggesting a metastability of this compound with respect to the stable phases.

The unit cells of $LiBH_4$, $LiNH_2$, $Li_2(BH_4)(NH_2)$ and $Li_4(BH_4)(NH_2)_3$ contains 4, 8, 18 and 8 molecules, with 3, 2, 6 and 4 set of non-magnetically equivalent hydrogens having a relative abundance of 4:4:8, 8:8, 6:6:6:6:6:6 and 24:24:24:8, respectively, as shown in *Table 2*. GIPAW calculation of chemical shifts outline a good agreement between the experimental and the weighted average value of computed chemical shift for each crystal structure.

In order to compare the experimental HP_DSC data with ab-inition calculations, a $LiBH_4$-$LiNH_2$ pseudo-binary phase diagram was calculated according to the Calphad approach. Experimental data and output of ab-initio calculations available in the literature, as well as obtained in this work, have been used as input. Available thermodynamic databases [36] and literature data [31] have been used as a starting point for the calculation and thermodynamic functions not available have been assessed. A value of -11.2 kJ/mol, estimated through ab-initio calculations for the reaction enthalpy for $LiBH_4$+3$LiNH_2$ -> $Li_4(BH_4)(NH_2)_3$ [35], was used to determine the GFE of the 1:3 compound. Since only solid phases are involved in this reaction, the entropy difference was assumed to be negligible. The experimental temperature and enthalpy of melting for pure $LiNH_2$ (T_m = 357 °C, ΔH_m = 14.3 kJ/mol), asobtained by calorimetriyin the present work, were used as input to describe the Gibbs energy of the liquid phase. Considering a regular solution model to describe the liquid

mixture between $LiNH_2$ and $LiBH_4$, an interaction parameter Ω_{liquid} = -13.0 kJ/mol was obtained from the assessment. Results of the calculation are shown in *Figure 6*, together with experimental data of relevant temperatures of HP_DSC peaks, as evidenced in *Figure 3*. It is worth noting that, according to the calculations, a peritectic melting is predicted for the $Li_4(BH_4)(NH_2)_3$ compound. Finally it must be underlined that, according to the results of this work and to recent experimental information [13,2], the $Li_2(BH_4)(NH_2)$ compound is metastable and, therefore, it is not present in the stable phase diagram.

Conclusions

In this work, $Li_2(NH_2)(BH_4)$ and $Li_4(NH_2)_3(BH_4)$ compounds have been prepared through various synthesis techniques i.e. ball milling, annealing treatment and quenching. XRD results have shown that a nearly single $Li_2(NH_2)(BH_4)$ phase can be only obtained by quenching of the liquid, whereas $Li_4(NH_2)_3(BH_4)$ can be easily obtained with all synthesis routes. HP_DSC experiments allowed following the formation of the compounds, providing experimental data for the phase transformations. Solid-state nuclear magnetic resonance experiments on quenched samples confirmed the presence of the compounds, providing information on the environment of various nuclei. Ab-initio calculations gave good agreement between experimental and the optimized lattice parameters and chemical shifts. The enthalpy of formation of $Li_2(BH_4)(NH_2)$ and $Li_4(BH_4)(NH_2)_3$ compounds from $LiBH_4$ + $LiNH_2$ mixtures turned out equal to -6.6 and -13.9 kJ/mol, respectively. A Calphad assessment of the $LiBH_4$-$LiNH_2$ pseudo binary phase diagram has been obtained, considering a regular solution model for the liquid phase. A good agreement between experimental and calculated temperatures for phase transformations has been obtained.

Results obtained in this work suggests that $Li_2(BH_4)(NH_2)$ compound is formed as a metastable phase with respect to the stable equilibrium mixture. In addition, a peritectic melting for the $Li_4(BH_4)(NH_2)_3$ phase has been established.

Acknowledgements

Antonio Santoru (HZG – Helmholtz-Zentrum Geesthacht – Germany) is kindly acknowledged for support in ball milling experiments. The research leading to these results has received funding from the European Marie Curie Actions under ECOSTORE (www.ecostore-itn.eu) grant agreement n°607040.

References

[1] B.Sakintuna, F. Lamari-Darkrim, M. Hirscher, *International Journal of Hydrogen Energy, 32, 1121,(2007).*

[2] A. Borgschulte, M. O. Jones, E. Callini, B. Probst, S. Kato, A. Züttel, W. I. F. David, S. Orimo, *Energy Environ. Sci., 5, 6823, (2012).*

[3] P.A. Chater, W.I.F. David, P.A. Anderson, *Chem. Commun., 45, 4770, (2007).*

[4] C. Liu, F. Li, L. P. Ma, H.-M. Cheng, *Adv. Mater., 22, E28, (2010).*

[5] M.Matsuo, Y.Nakamori, S.Orimo, H.Maekawa, H.Takamura, *Appl. Phys. Lett., 91, 224103, (2007).*

[6] M. Matsuo, T. Sato, Y. Miura, H. Oguchi, Y. Zhou, H. Maekawa, H. Takamura, S. Orimo, *Chem. Mater., 22, 2702, (2010).*

[7] R. A. Davies, D. R. Hewett, P. A. Anderson, *Adv. Nat. Sci.: Nanosci. Nanotechnol., 6, 015005, (2015).*

[8] M. Matsuo, A. Remhof, P. Martelli, R. Caputo, M. Ernst, Y. Miura, T. Sato, H. Oguchi, H. Maekawa, H. Takamura, A. Borgschulte, A. Züttel, S.I. Orimo, *J. Am. Chem. Soc., 131,16389, (2009).*

[9] M. Matsuo, S. Orimo, *Adv. Energy Mater., 1, 161, (2011).*

[10] T. Noritake, M. Aoki, S. Towata, A. Ninomiya, Y. Nakamori, S. Orimo, *Appl. Phys. A, 83, 277, (2006).*

[11] Y. Zhou, M. Matsuo, Y. Miura, H. Takamura, H. Maekawa, A. Remhof, A. Borgschulte, A. Zuttel, T. Otomo, S. Orimo, *Materials Transactions, 52, 654, (2011).*

[12] G. P. Meisner, M. L. Scullin, M. P. Balogh, F. E. Pinkerton, M. S. Meyer, *J. Phys. Chem. B., 110, 4186, (2006).*

[13] J. P. Singer, M. S. Meyer, R. M. Speer, Jr., J. E. Fischer, F. E. Pinkerton, *Phys. Chem. C, 113,18927,(2009).*

[14] P. A. Anderson, P. A. Chater, W. I. F. David, I. C. Evans, A. L. Kersting, *Mater. Res. Soc. Symp. Proc., 1216, W09-05, (2010).*

[15] L. Lutterotti, S. Matthies, H. R. Wenk, *"MAUD: a friendly Java program for material analysis using diffraction." IUCr: Newsletter of the CPD 21.14-15, (1999).*

[16] P. Giannozzi, S.Baroni, N.Bonini, M. Calandra, R. Car, C. Cavazzoni, D.Ceresoli, G. L.Chiarotti, M.Cococcioni,I.Dabo, A. Dal Corso, S. de Gironcoli, S. Fabris, G.Fratesi, R.Gebauer,U.Gerstmann,C.Gougoussis, A.Kokalj, M.Lazzeri, L. Martin-Samos, N.Marzari, F. Mauri, R. Mazzarello, S.Paolini, A.Pasquarello, L.Paulatto, C.Sbraccia, S.Scandolo, G. Sclauzero, A. P.Seitsonen, A. Smogunov, P. Umari, R. M.Wentzcovitch, *J. Phys. : Condens. Matter, 21, 395502, (2009).*

[17] a) J. Perdew, K. Burke, M.Ernzerhof, *Phys. Rev. Lett.,77, 3865, (1996);* b) J. P. Perdew, Y. Wang, *Phys. Rev. B,33, 8800, (1986).*

[18] a) A. Otero-de-la Roza, E. R. Johnson, *J. Chem. Phys.,138, 204109,(2013);* b) A. Otero-de-la Roza, E. R. Johnson, G. A.DiLabio, *J. Chem. Theory Comput., 10, 5436, (2014).*

[19] J. P. Soulie, G.Renaudin, R. Cerny, J.Yvon, *J.Alloys Compd., 346, 200, (2002).*

[20] a) H. Jacobs, R. Juza, *Z. Anorg. Allg. Chem., 391, 271, (1972);* b) J. B. Yang, X. D. Zhou,Q. Cai, W. J. James, W. B. Yelon, *Appl. Phys. Lett., 88, 041914, (2006).*

[21] H. Wu, W. Zhou, T. J. Udovic, J. J. Rush, T. Yildirim, *Chem. Mater., 20, 1245, (2008).*

[22] G. Kresse, D.Joubert, *Phys. Rev. B, 59, 1758, (1999).*

[23] H. J. Monkhorst, J.D. Pack, *Phys. Rev. B, 13,5188, (1976).*

[24] F. Franco, M. Baricco, M. R. Chierotti, R. Gobetto, C. Nervi, *J. Phys. Chem. C, 117, 9991, (2013).*

[25] C. J. Pickard, F. Mauri, *Phys. Rev. B, 63, 245101, (2001).*

[26] R. Gobetto, C. Nervi, E.Valfre, M.R. Chierotti, D. Braga, L. Maini, F. Grepioni, R.K. Harris, P. Y.Ghi, *Chem. Mater.***,** *17,1457, (2005).*

[27] H. L. Lukas, S. G. Fries, B. Sundman, *Computational Thermodynamics Cambridge University Press, (2007).*

[28] P.A. Chater, W.I.F. David, S.R. Johnson, P.P. Edwards, P.A. Anderson, *Chem. Commun., 23, 2439, (2006).*

[29] J. Yang, X. J. Wang, Q. Cai, W. B. Yelon, W. J. James, *Journal of Applied Physic 102, 0033507, (2007).*

[30] Y. E. Filinchuk, K. Yvon, G. P. Meisner, F. E. Pinkerton, M. P.Balogh, *Inorg Chem., 45, 1433, (2006).*

[31] A. El Kharbachi, E. Pinatel, I. Nuta, M. Baricco, *CALPHAD: Computer Coupling of Phase Diagrams and Thermochemistry, 39, 80, (2012).*

[32] T. Izuhara, H. T. Takeshita, H. Miyake, *J. Japan Inst. Metals, 75, 115 , (2011).*

[33] R. L. Corey, D. T, Shane, R. C. Bowman, Jr., M. S. Conradi, *J. Phys. Chem. C,112, 18706, (2008);* b) O. Dolotko, H. Zhang, O. Ugurlu, J. W. Wiench, M. Pruski, L. S. Chumbley, V. Pecharsky,*Acta Materialia, 55, 3121, (2007).*

[34] J. F. Herbsta, L. G. Hector, Jr., *Appl. Phys. Lett., 88, 231904, (2006).*

[35] D. J. Siegel, C. Wolverton, V.Ozoliņš, *Physical Review B, 75, 014101, (2007).*

[36] SGTE, Substances Database v 4.1.

Figure captions

Figure 1.XRD patterns for samples obtained from BM, AT and QU synthesis route for 1:1 (*a*) and 1:3 (*b*) $LiBH_4$:$LiNH_2$ mixture. Points: experimental data; lines: Rietveld fit. Peak position of various phases are shown in the bottom. For each pattern, the corresponding values of phase fraction in wt % are displayed, where 1:1 is $Li_2(NH_2)(BH_4)$ and 1:3 is $Li_4(NH_2)_3(BH_4)$ compound.

Figure 2. HP_DSC traces (red – 1st cycle, blue – 2nd cycle) for 1:1 (*a*) and 1:3 (*b*) $LiBH_4$:$LiNH_2$ mixtures.

Figure 3. HP_DSC traces of $(LiBH_4)_{1-x}(LiNH_2)_x$ mixtures (x = 0.00, 0.15, 0.33, 0.50, 0.65, 0.75, 0.85, 1.00). Points indicaterelevant transition temperatures used for phase diagram assesment. Peaks marked with sign '*x*' correpond to melting of $Li_2(NH_2)(BH_4)$ phase. Peaks marked with '*y*' correpond to the formation of $Li_4(NH_2)_3(BH_4)$ phase.

Figure 4. ^{1}H (400.23 MHz) MAS (top) and ^{15}N (40.56 MHz) CPMAS (bottom) spectra of $LiNH_2$, $LiBH_4$, 1:1 and 1:3 QU mixtures, recorded with a spinning speed of 32 and 9 kHz, respectively. Blue, red and green dotted lines in the ^{1}H spectra of 1:1 and 1:3 mixtures represent the NH_2^-, BH_4^- and unreacted $LiNH_2$ component, respectively as obtained from deconvolution analysis.

Figure 5. ^{7}Li (155.54 MHz) MAS (top) and ^{11}B (128.41 MHz) MAS (bottom) spectra of $LiNH_2$, $LiBH_4$, 1:1 and 1:3 mixtures, recorded with a spinning speed of 12 kHz, respectively.

Figure 6.Calculated $LiBH_4$-$LiNH_2$ pseudo-binary phase diagram (solid lines). Experimental data (points), as shown on *Figure 3*, are also reported for comparison.

Table 1. Experimental and computed structural parameters for $LiBH_4$, $LiNH_2$, $Li_2(BH_4)(NH_2)$ and $Li_4(BH_4)(NH_2)_3$ compounds.

		Experimental					Computed			
Compound	**Space group**	***a*(Å)**	***b*(Å)**	***c*(Å)**	**V (Å^3)**	**Ref**	***a*(Å)**	***b*(Å)**	***c*(Å)**	**V (Å^3)**
$LiBH_4$	P_{nma}	7.179	4.437	6.803	216.7	[19]	7.132	4.399	6.685	209.7
$LiNH_2$	*I*-4	5.037	5.037	10.278	260.8	[20]	5.037	5.037	10.282	260.8
$Li_2(BH_4)(NH_2)$	*R*-3	14.394 14.489 14.490 14.456 14.449 14.457	14.394 14.489 14.490 14.456 14.449 14.457	9.052 9.340 9.240 9.206 9.218 9.226	1624.2 1698.1 1680.1 1666.1 1662.2 1669.9	[21] [3] [10] BM AT QU	14.403	14.403	9.062	1628.0
$Li_4(BH_4)(NH_2)_3$	$I2_13$	10.665 10.656 10.645 10.679 10.666 10.657 10.656	10.665 10.656 10.645 10.679 10.666 10.657 10.656	10.665 10.656 10.645 10.679 10.666 10.657 10.656	1213.1 1210.0 1206.2 1217.8 1213.4 1210.3 1210.0	[21] [10] [28] [29] BM AT QU	10.621	10.621	10.621	1198.0

Table 2.Experimental and computed solid-state NMR parameters, δ = chemical shift, # = number of equivalent nuclei in the cell.

Compound		Exp δ	#	Averaged δ_{iso}	Computed δ_{iso}	δ_{11}	δ_{22}	δ_{33}
$LiBH_4$	^{1}H	–0.40	4	–0.20	–0.14	0.63	–0.24	–0.82
			4		–0.61	0.36	–0.22	–1.97
			8		–0.03	1.09	0.31	–1.48
	^{7}Li	–0.91	4	–0.91	–0.91	0.05	–0.74	–2.04
	^{11}B	–41.8	4	–41.80	–41.80	–39.14	–42.94	–43.34
$LiNH_2$	^{1}H	–1.4	8	–1.71	–1.53	4.34	2.36	–11.28
			8		–1.88	3.81	1.59	–11.05
	^{7}Li	2.4	2	3.69	3.32	4.38	2.78	2.78
			2		3.98	4.51	4.51	2.92
			4		3.73	5.08	3.77	2.34
	^{15}N	–18.6	2	–18.60	–18.64	–4.92	–15.33	–35.67
			2		–18.59	–4.98	–15.50	–35.30
			2		–18.57	–5.06	–15.19	–35.47
			2		–18.61	–4.80	–15.55	–35.48
$Li_2(BH_4)(NH_2)$	^{1}H	–0.2	6	–0.37	0.12	1.64	1.48	0.53
			6		0.35	2.17	0.06	–1.16
			6		–1.56	2.45	1.37	–8.50
			6		–1.34	3.19	2.97	–10.20
			6		0.11	0.43	0.05	–0.16
			6		–0.28	1.35	–0.67	–1.53
	^{7}Li	0.9	18	1.45	0.88	3.87	1.70	–2.94
			18		2.02	5.01	2.84	–1.80
	^{11}B	–39.6	6	–39.54	–39.53	–34.75	–38.87	–44.98
			6		–39.54	–34.76	–38.87	–45.00
			6		–39.55	–34.76	–38.90	–44.98
	^{15}N	–24.1	6	–25.42	–25.39	–13.28	–24.27	–38.62
			6		–25.41	–13.38	–24.25	–38.59
			6		–25.45	–13.35	–24.29	–38.71
$Li_4(BH_4)(NH_2)_3$	^{1}H	–0.2	24	–0.98	–0.35	0.39	0.16	–1.61
			24		–1.47	3.81	2.47	–10.71
			24		–1.61	3.44	1.91	–10.18
			8		0.53	1.22	1.22	–0.85
	^{7}Li	1.80	12	3.64	2.37	8.06	2.11	–3.05
			12		3.69	5.01	3.31	2.74
			8		2.13	6.22	0.09	0.09
	^{11}B	–40.2	8	–41.46	–41.46	–34.99	–44.70	–44.70
	^{15}N	–20.6	24	–20.94	–20.94	–7.48	–22.61	–32.75

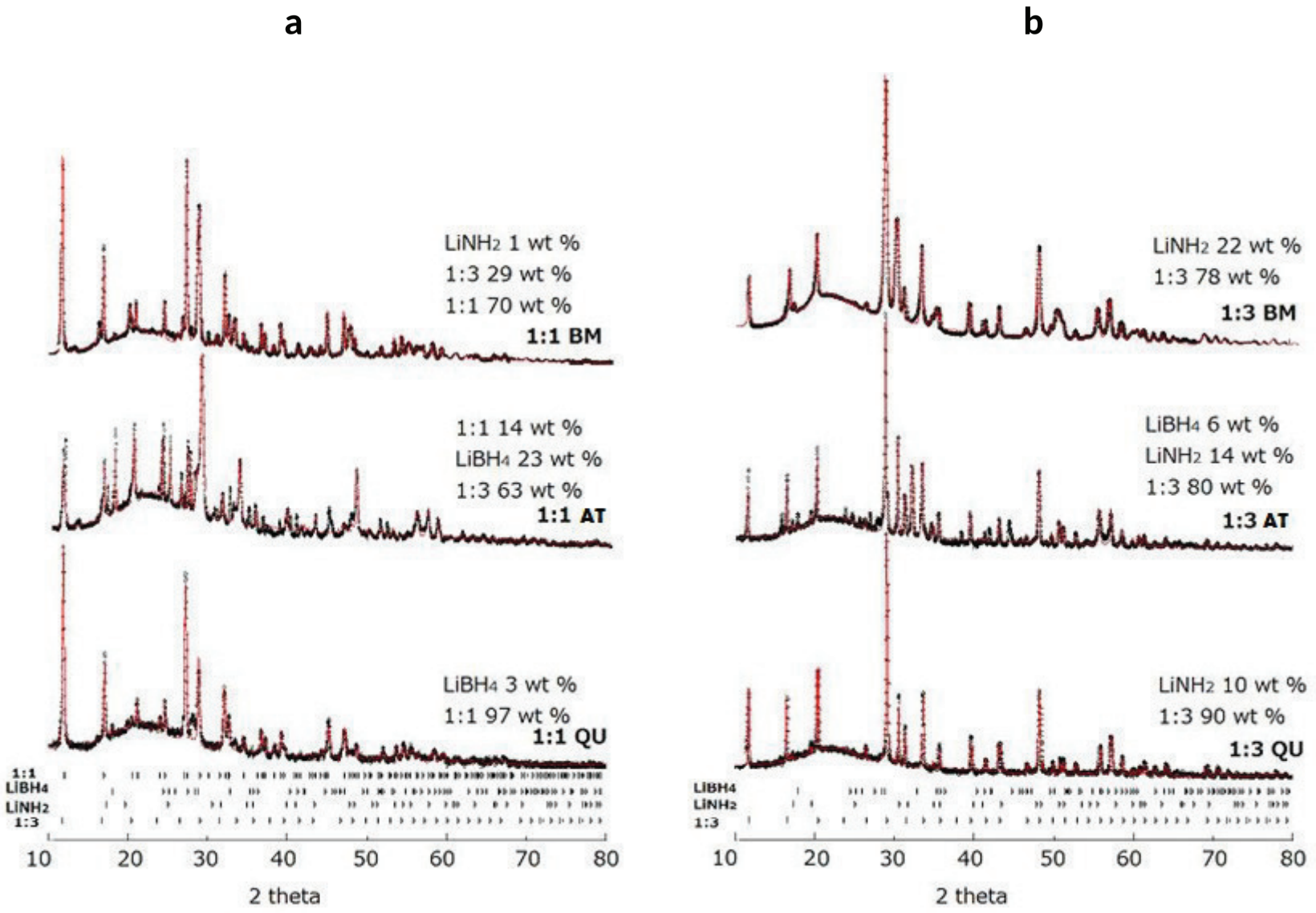

Wolczyk et.al . Figure 1

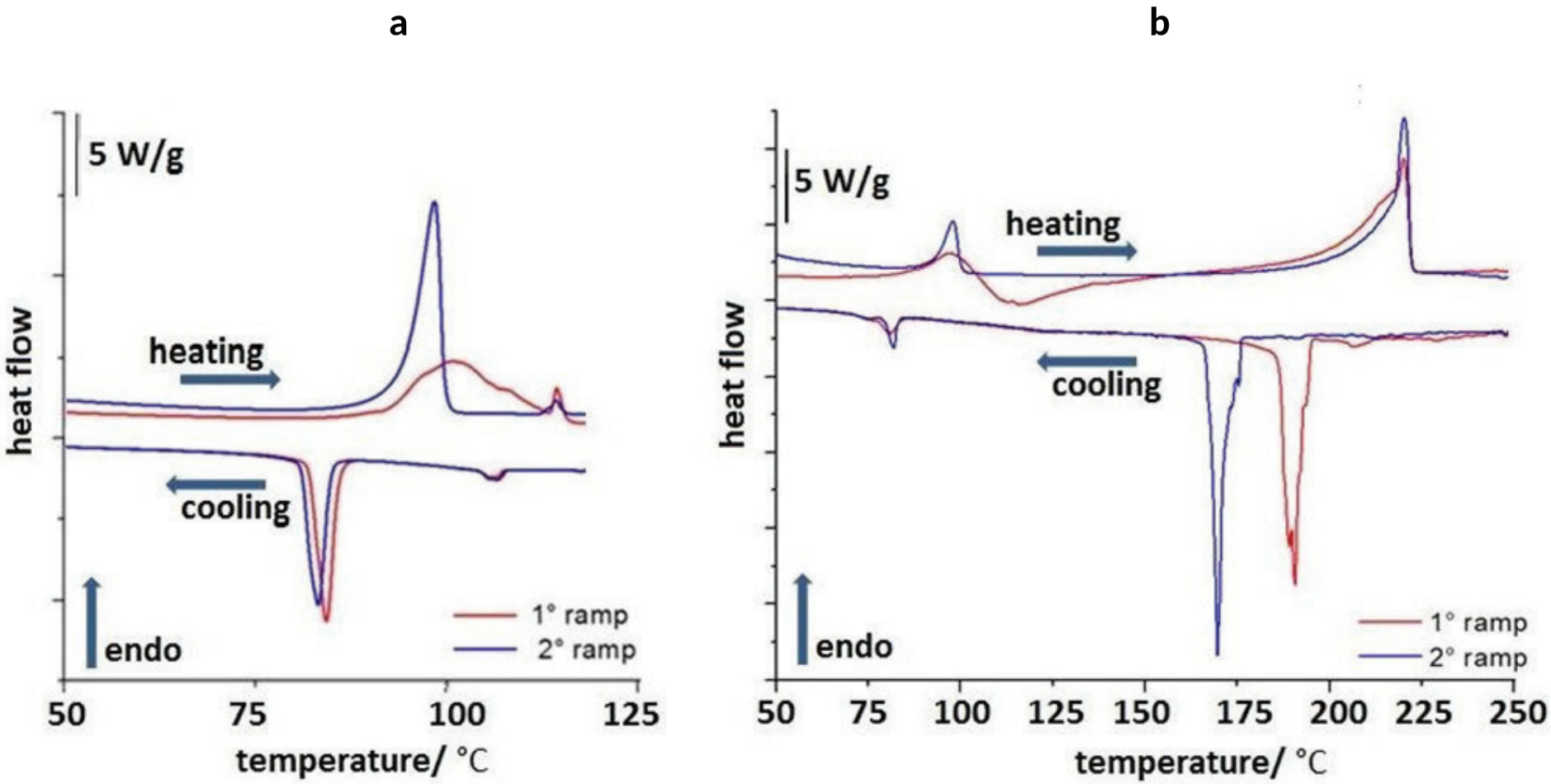

Wolczyk et.al . Figure 2

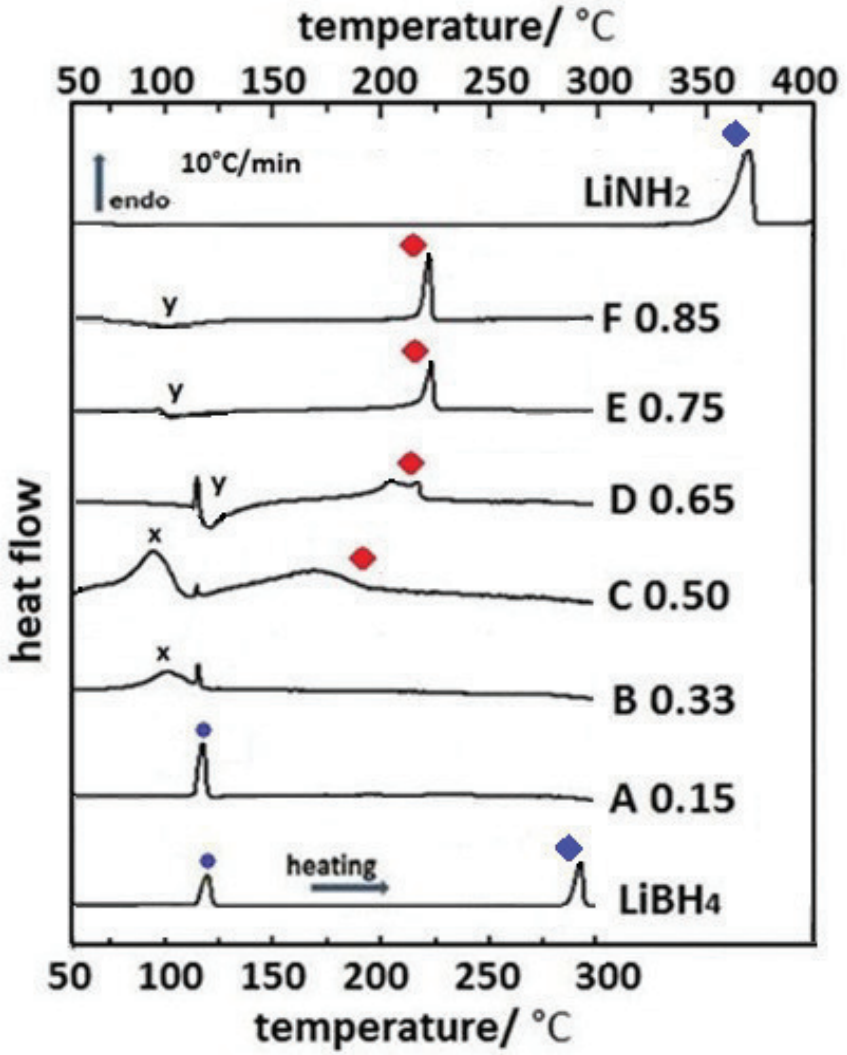

Wolczyk et.al . Figure 3

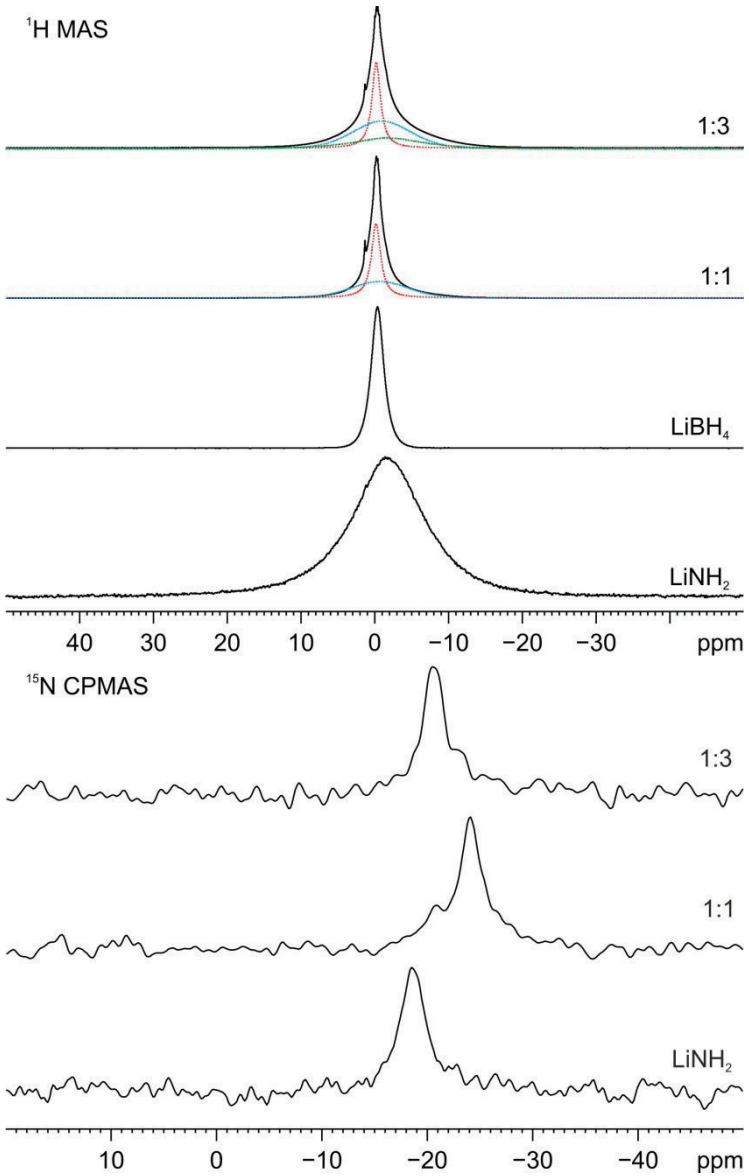

Wolczyk et.al . Figure 4

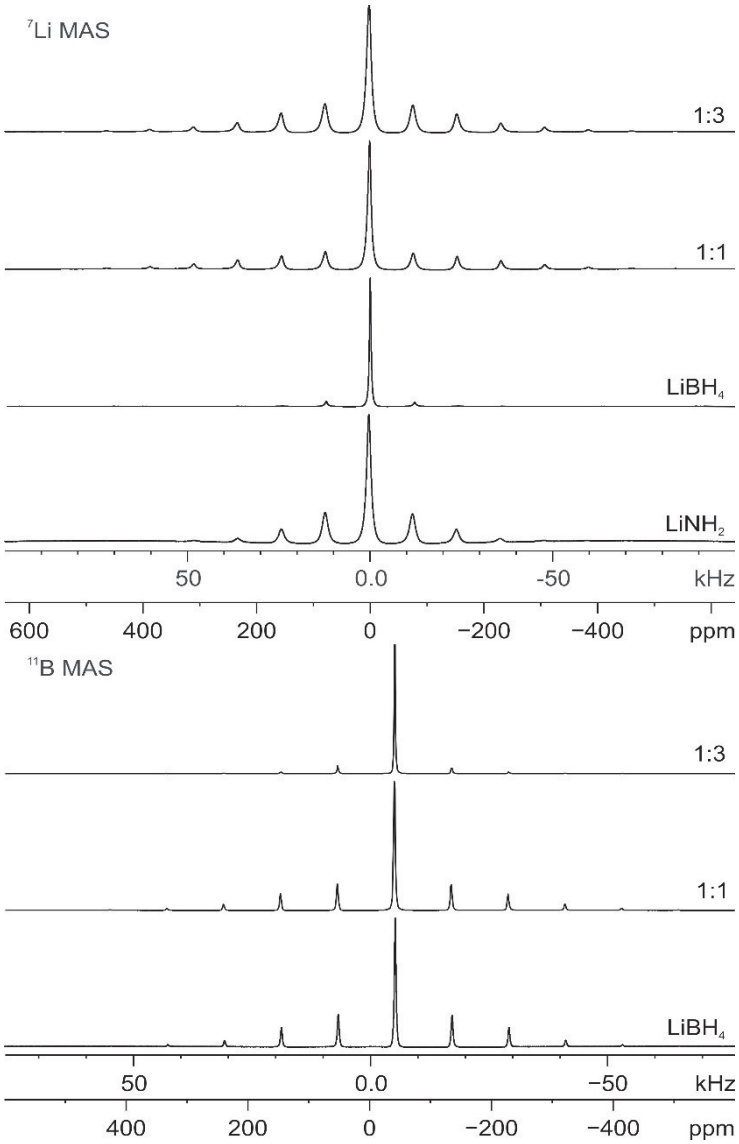

Wolczyk et.al . Figure 5

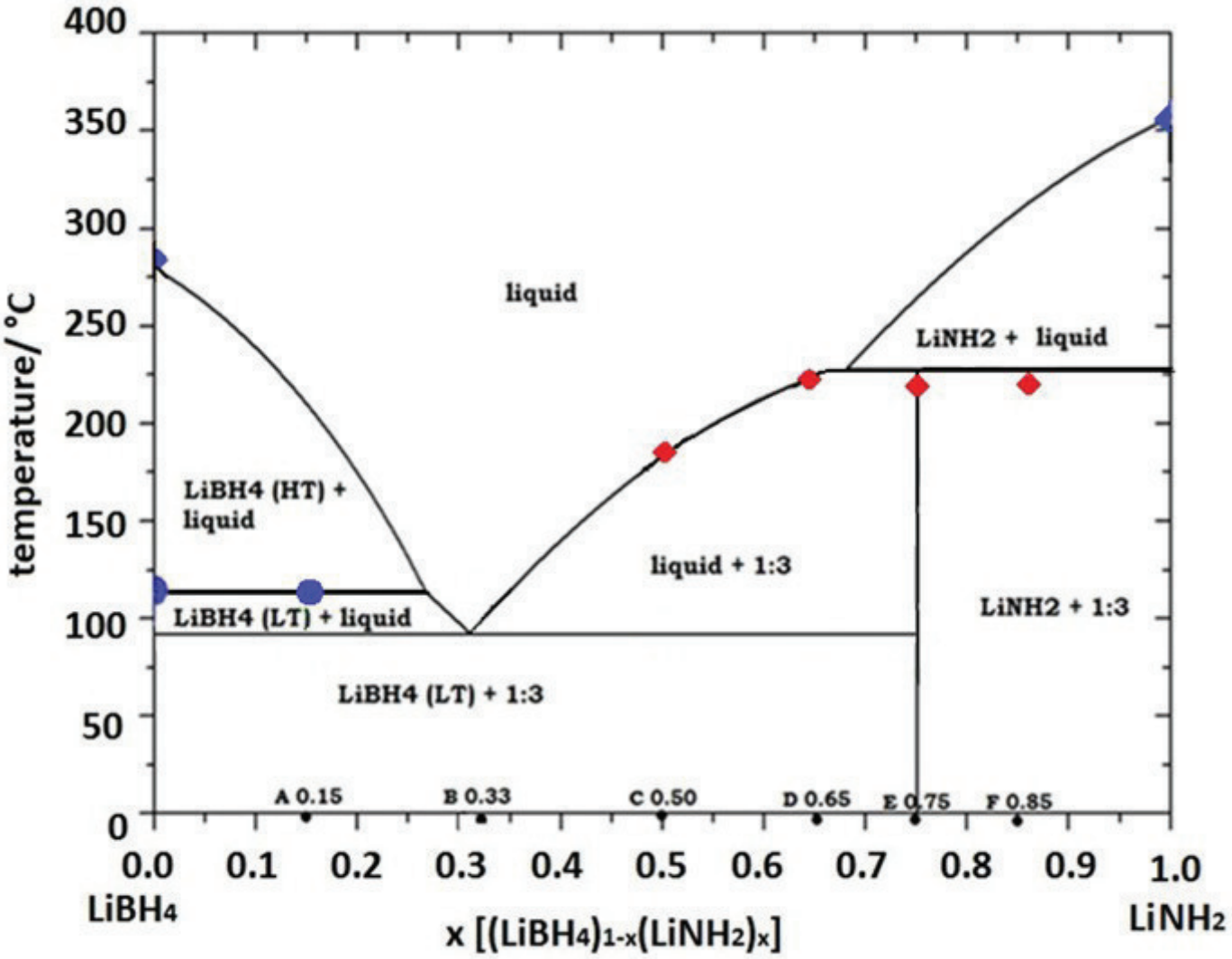

Wolczyk et.al . Figure 6

Highlights

- $Li_2(NH_2)(BH_4)$ and $Li_4(NH_2)_3(BH_4)$ compounds prepared by ball milling, annealing treatment and quenching. Single $Li_2(NH_2)(BH_4)$ phase obtained by quenching, whereas $Li_4(NH_2)_3(BH_4)$ easily obtained with all synthesis routes.
- HP_DSC experiments allowed following the formation of the compounds, providing experimental data for the phase transformations.
- Solid-state nuclear magnetic resonance experiments on quenched samples confirmed the presence of the compounds, providing information on the environment of various nuclei.
- Ab-initio calculations gave good agreement between experimental and the optimized lattice parameters and chemical shifts.
- A Calphad assessment of the $LiBH_4$-$LiNH_2$ pseudo binary phase diagram has been obtained.
- $Li_2(BH_4)(NH_2)$ compound is formed as a metastable phase and a peritectic melting for the $Li_4(BH_4)(NH_2)_3$ phase has been established.